

Breakup of Spiral Waves into Chemical Turbulence

S. M. Tobias

JILA, University of Colorado, Boulder, Colorado 80309

E. Knobloch

Department of Physics, University of California, Berkeley, California 94720

(Received 23 September 1997)

Recent experiments on spiral waves in the Belousov-Zhabotinsky reaction indicate that the waves may break up sufficiently far from the core into chemical turbulence. Simulations of target patterns in the FitzHugh-Nagumo and Ginzburg-Landau models indicate that such transitions occur when the wave frequency pushes the selected wave vector into the regime of *absolute* Eckhaus instability. This frequency in turn depends on the control parameter and boundary conditions through the solution of a nonlinear eigenvalue problem. [S0031-9007(98)06192-4]

PACS numbers: 82.40.Ck, 47.27.-i, 47.54.+r

Complex spatiotemporal dynamics are found in many continuous systems of physical interest [1]. In oscillatory systems this behavior often takes the form of defect-mediated turbulence [2]. In one dimension these defects are called *holes* [1,3]; in two dimensions they take the form of *spirals* [1,3], and *shock vertices* [4]. Thus far the resulting complex dynamics have been studied primarily within the complex Ginzburg-Landau (CGL) equation [1,2], although similar dynamics have been found in many reaction-diffusion systems [5]. In two dimensions elementary solutions of the CGL equation in the form of uniformly rotating spirals are well known. These solutions carry a net topological charge and rotate with a frequency Ω determined by the solution of a nonlinear eigenvalue problem [6]. This frequency in turn selects the radial wave vector and amplitude, and thus controls the global structure of the spiral. Recent experiments on the Belousov-Zhabotinsky (BZ) reaction by Ouyang and Flesselles [7] indicate that the resulting spiral may break up into a turbulent region outside of a laminar core, a behavior they attribute to the presence of a convective Eckhaus instability. We show below that in systems of finite aspect ratio L , however large, an instability of the observed type occurs only in the regime of *absolute* Eckhaus instability. This distinction is critical because in the convectively unstable regime disturbances undergo transient amplification as they propagate but must ultimately decay. In contrast, the absolute instability regime is characterized by the presence of a globally unstable mode. This mode is typically a wall mode confined to the outer boundary; the resulting instability moves in from the boundary as the control parameter μ increases beyond threshold, and forms a *front* separating the laminar inner spiral from the turbulent outer regions, as in the experiments [7]. We confirm these conclusions with simulations of the CGL and FitzHugh-Nagumo models.

Consider first the CGL model [3]

$$A_t = \mu A + (1 + ib)\nabla^2 A - (1 + ic)|A|^2 A \quad (1)$$

in one and two dimensions, where b, c are real coefficients satisfying $1 + bc > 0$, and μ is the control parameter. If (1) is posed on the whole real line, μ can be scaled away. On a finite domain, or one on which periodic boundary conditions (PBC) are imposed, this is no longer so. In the following we fix the domain size L , and increase μ .

In two dimensions the direction of propagation of the wave fronts (outward or inward) is determined by the frequency Ω through the radial wave vector. This directionality is critical to much of the subsequent behavior. To appreciate its role consider the one-dimensional CGL with $A_x(0) = A(L) = 0$ and a group velocity term $v_g A_x$, $v_g > 0$, added to the left hand side. This problem provides a simple model of the breakup process, with $x = 0$ playing the role of the core and $x = L$ the outer boundary. The condition $A_x(0) = 0$ is necessary in order that the resulting solution represent a solution of (1) on the full domain $-L < x < L$. Within this model the trivial state becomes convectively unstable to right-propagating waves at $\mu = 0$. For $0 < \mu < \mu_f(L)$ these waves exhibit transient growth, but eventually decay because they cannot be reflected from $x = L$ [8]. As a result in a finite domain a *sustained* wave is possible only for $\mu > \mu_f(L) = \mu_a + \mathcal{O}(L^{-2})$ for $L \gg 1$. Here $\mu_a \equiv v_g^2/4(1 + b^2)$ is the threshold for the transition to *absolute* instability, computed for an unbounded domain [8]. For $\mu_f < \mu < \mu_f + \mathcal{O}(L^{-5})$ this wave is a wall mode attached to $x = L$ with $\mathcal{O}(v_g/(1 + b^2))$ decay length; for $\mu = \mu_f + \mathcal{O}(L^{-2})$ it becomes a fully nonlinear wave, with a stationary front at $x = x_1$ separating a small amplitude *core* solution from an $\mathcal{O}(1)$ amplitude wave in $x_1 < x < L$ [9,10]. This front moves inward with increasing μ . In the absence of phase slips at the front the wave number in the post-front region is selected by the frequency of the wave in the core region. If μ is not too large and $L \gg 1$ this frequency is $\Omega \approx \omega_a \equiv b v_g^2/4(1 + b^2)$. For larger μ the frequency Ω solves a nonlinear eigenvalue problem [9] and begins to depart substantially from ω_a , and the selected wave

number can change sign or be pushed into an Eckhaus unstable regime. In an unbounded domain the Eckhaus instability is convective [11]. As a consequence the growing disturbances are advected towards the boundary at $x = L$ and ultimately decay unless the threshold for *absolute* Eckhaus instability is exceeded, just as for the primary instability [10]. The evolution of this instability nucleates defects [12] and can lead to either defect-mediated turbulence [2] or a secondary wave train with a different (and stable) wave number. Both types of behavior have been observed [10], and are robust with respect to changing the boundary conditions, provided there are no incoming waves from $x < 0$ [8]. In Fig. 1 we show the critical frequency Ω_{ae} of the basic wave train at the onset of absolute Eckhaus instability as a function of b and c when $v_g = 1.0$. The instability is present for $\Omega > \Omega_{ae}$. This critical frequency is insensitive to the core boundary condition. For example, μ_{ae} (the critical value of μ at which the secondary instability sets in) was found to vary by less than 0.1% when the core boundary condition was changed to $A(0) = 0$.

In two dimensions Eq. (1) has axisymmetric solutions called target patterns. In these solutions, which can be computed with the boundary conditions $A(0) = A(L) = 0$, the $r^{-1}A_r$ term in $\nabla^2 A$ plays the role of the drift term added to Eq. (1) when discussing the 1D problem, and is responsible for the presence of a preferred direction of propagation (Fig. 2). Consequently, our picture of target formation is essentially the same as in the 1D problem, except that μ_a is now itself of order L^{-2} : a target forms when the threshold for primary absolute instability is exceeded. In large domains the resulting pattern becomes nonlinear almost immediately, and an exponential front forms separating the core from the visible [i.e., $\mathcal{O}(1)$ amplitude] waves. As in the 1D case the frequency selects both the radial wave number and the amplitude of the waves outside of the core, as illustrated in Figs. 2 and 3. These results

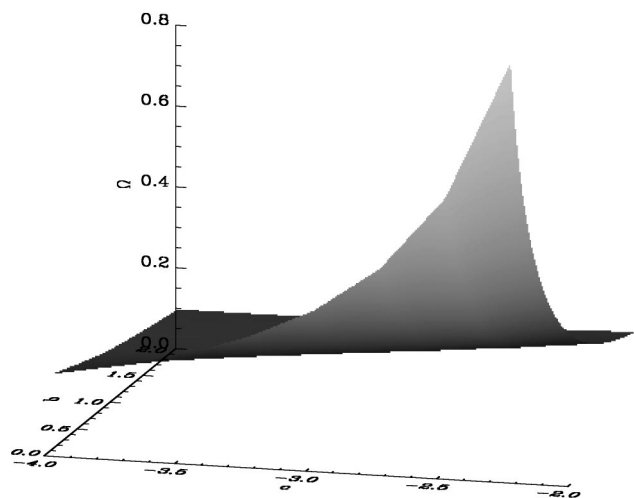


FIG. 1. The frequency Ω_{ae} of the primary wave train at the onset of absolute Eckhaus instability in the CGL equation in one dimension as a function of the coefficients b, c , for $L = 60$ and $v_g = 1.0$.

represent time-asymptotic states, i.e., states of the system after transients [whose duration is at least $\mathcal{O}(L)$] have died away. For the parameter values used the wave number of the basic target pattern is positive, i.e., the waves travel inward. If this wave number lies in the region of absolute Eckhaus instability the evolution of the resulting instability leads to defect-mediated turbulence of the type seen

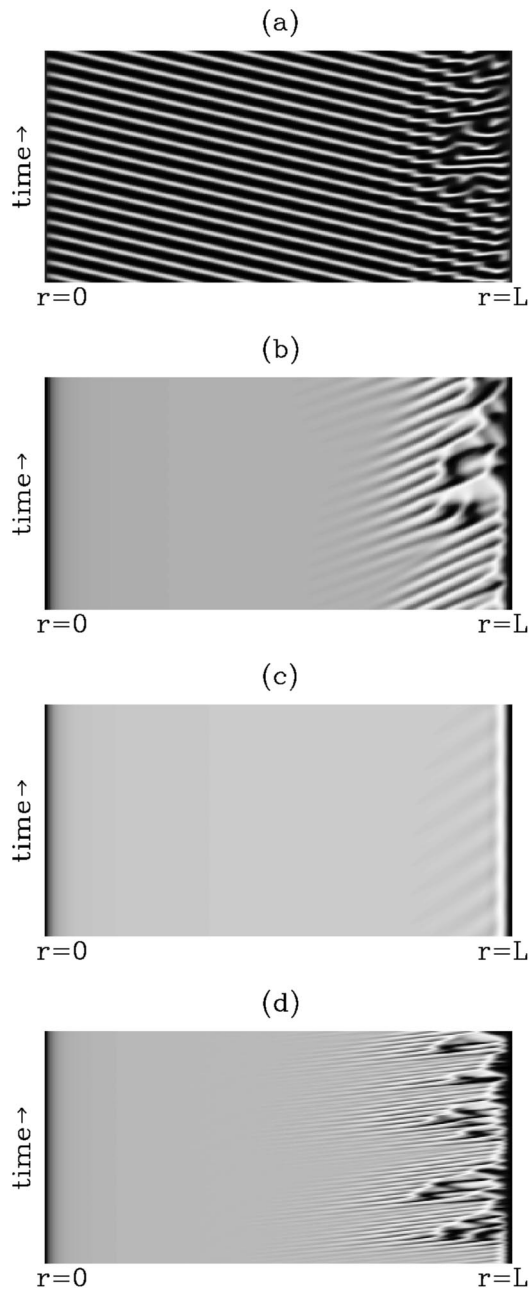


FIG. 2. The breakup of a target pattern via absolute Eckhaus instability obtained from the axisymmetric CGL Eq. (1) for $\mu = 3.5, b = 0.45, c = -2.0$, and $L = 60$. The space-time plots of (a) $\text{Re}[A(r, t)]$, (b) $|A(r, t)|$ reveal a front separating a laminar region of (ingoing) waves from a turbulent region near $r = L$. The meandering of the front is clearly visible. (c) $|A(r, t)|$ for $\mu = 3.0$ with no noise and (d) $|A(r, t)|$ for $\mu = 3.0$ and noise strength $\sigma = 10^{-3}$, showing that at $\mu = 3.0$ the Eckhaus instability is convective.

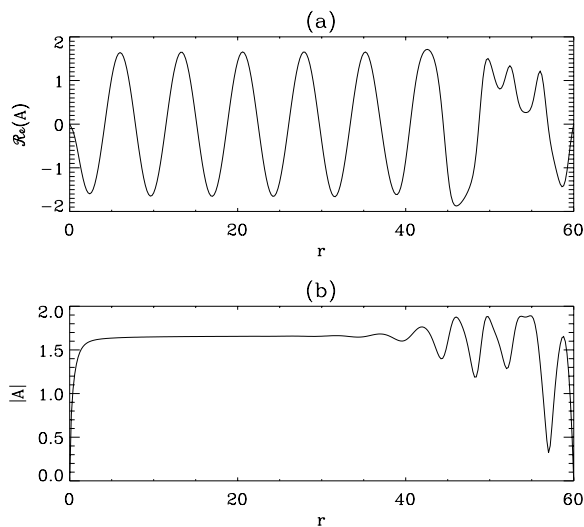


FIG. 3. Target solutions (a) $\text{Re}[A(r, t)]$, (b) $|A(r, t)|$ of the CGL equation (1) at a particular instant in time. The parameters are $\mu = 3.5$, $b = 0.45$, $c = -2.0$, and $L = 60$.

experimentally [7] and found numerically in Eq. (1) with no-flux boundary conditions [7]. As in the 1D case this instability appears first at $r = L$; once this threshold is exceeded the secondary front separating the inner (laminar) behavior from the outer (turbulent) behavior moves inwards with increasing μ . This is clearly visible in Fig. 2(b), which shows a laminar wave train in $0 \approx r_1 < r < r_2$ acquiring wave number and frequency modulation near $r = r_2$ and its subsequent breakup into turbulence with increasing modulation amplitude beyond $r = r_2$. The “corrugations” visible in Fig. 2(a) near the front are a consequence of the outward phase velocity of this modulation. Such spatially growing modulation of the basic wave number on the laminar side of the front was observed in the experiments [7]. In the present case the front itself is not stationary but meanders about a mean position that depends on the system parameters. Except for the emphasis on the global aspects of the process of spiral breakup through its dependence on the frequency and the role played by the directionality of the waves in delimiting the regime of absolute Eckhaus instability the above picture is fundamentally that put forward in Ref. [13]. In particular the instability is associated, at threshold, with a complex modulation wave number k . The real part of this wave number describes radial modulation of the target; the instability first appears at $r = L$ because $\text{Re}(k) < 0$. The amplitude of this modulation increases exponentially with r with an e -folding distance given by $2\pi/\text{Im}(k)$. In other words, the presence of the laminar region is not a manifestation of a convective instability, rather it is a consequence of an absolute instability with a complex modulation wave number. This means that the laminar region is stable with respect to infinitesimal noise, and does not act as a noise amplifier as it would in a truly convectively unstable situation. In contrast at $\mu = 3.0$, before the onset of absolute instability, the injection of noise of rms ampli-

tude $\sigma = 10^{-3}$ results in noise-sustained turbulence near $r = L$ [Fig. 2(d)] but no such structure is present when $\sigma = 0$ [Fig. 2(c)]. Thus at $\mu = 3.0$ no global mode is present and the Eckhaus instability is *convective*. It follows that the presence of convective instability does *not* guarantee instability in a finite domain.

A useful model of the phenomena exhibited by the BZ reaction is provided by the FitzHugh-Nagumo model [14]

$$u_t = -\frac{1}{\epsilon} u(u-1) \left[u - \frac{v+b}{a} \right] + \nabla^2 u, \quad (2)$$

$$v_t = u - v.$$

In Fig. 4 we show the results of integrating an axisymmetric version of this model subject to the boundary conditions $u(0) = v(0) = 0$, $u_r(L) = v_r(L) = 0$. The figure shows the breakup of a target pattern as ϵ increases for $a = 0.2$, $b = -0.3$. Although in this case it is substantially harder to analyze the far-field instability of the resulting target, the figure indicates that the secondary instability manifests itself in the same way as in the CGL model: the secondary instability sets in first at $r = L$ and subsequently forms a (secondary) front separating a laminar inner region from the disordered outer region. The location of this front oscillates quite widely on a time scale that is much longer than the period of the basic target pattern. Moreover, corrugations corresponding to the modulation of the basic wave number are visible to the left of the front in Fig. 4(b), much as in the CGL example. In Fig. 5 we show the time-averaged location of the onset of spatial modulation as a function of ϵ , defined as the location where the solution differs in amplitude from the basic time-periodic state found in the laminar region by more than 1%. The front at $r_2 \approx 0.45L$ separates a region of constant wave number ($r < r_2$) from that with fluctuating

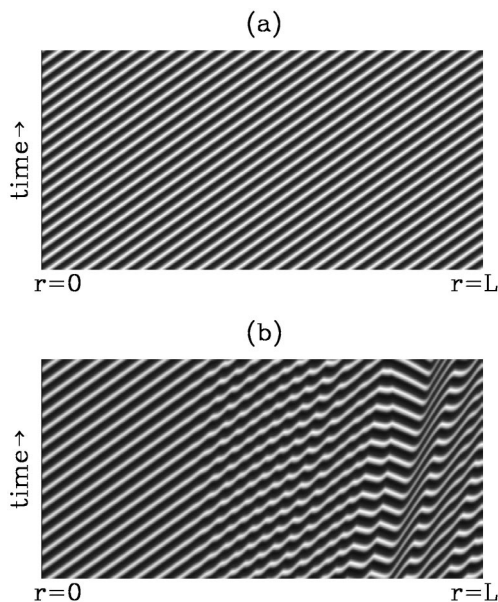


FIG. 4. Space-time diagrams showing target solutions $u(r, t)$ of (2) with $a = 0.2$, $b = -0.3$, and $L = 400.0$, showing the formation of the secondary front. (a) $\epsilon = 0.05$; (b) $\epsilon = 0.08$.

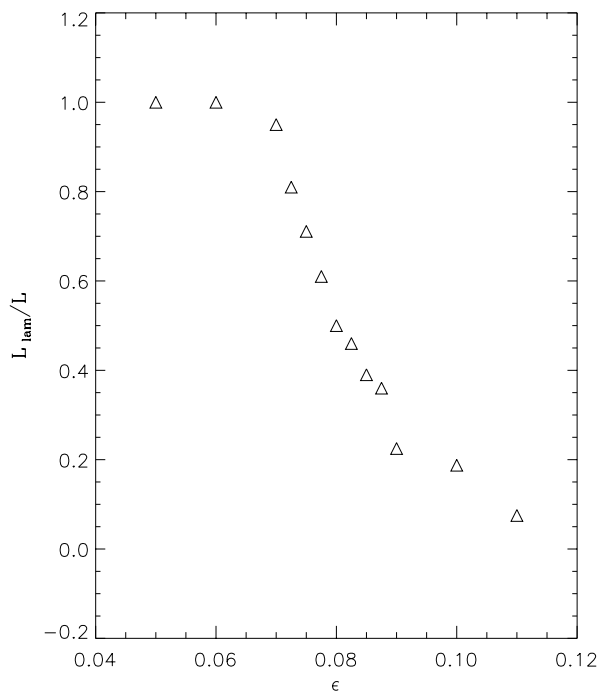


FIG. 5. Time-averaged distance from the core at $r = 0$ of the onset of spatial modulation in Fig. 4 as a function of ϵ .

wave number ($r > r_2$), cf. Fig. 4(b). The importance of the boundary conditions and of the r^{-1} term is indicated in Fig. 6, which shows the result of integrating Eqs. (2) in 1D with PBC. This problem lacks the preferred directionality of the 2D problem and the results differ completely from those shown in Fig. 4; in particular, no secondary front separating laminar and turbulent regions appears.

In finite domains unstable modes must set in as global eigenmodes. In large domains the threshold for the ap-

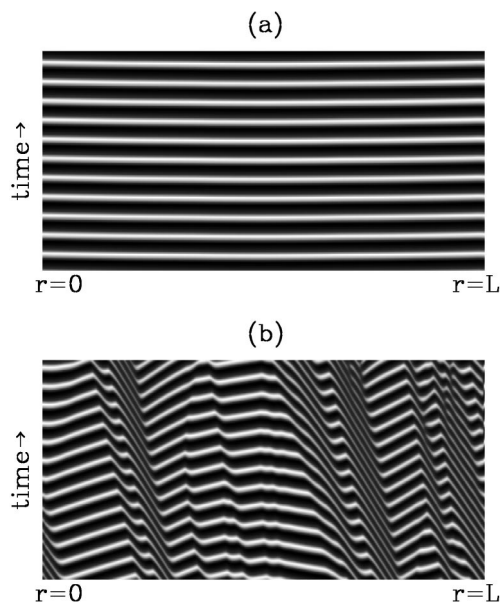


FIG. 6. Space-time diagrams showing solutions of Eqs. (2) in 1D with PBC, for comparison with Fig. 4. The parameter values are as in Figs. 4(a),4(b).

pearance of such global modes approximates the threshold for absolute instability, computed in the absence of boundaries. Below this threshold, i.e., in the regime traditionally referred to as convectively unstable, all disturbances undergo transient growth but ultimately decay. This is so regardless of the boundary conditions provided these prevent the replenishment of the disturbances from the “upstream” direction and is a consequence of the unidirectionality of the waves [8]. In the case of target patterns the core at $r = 0$ supplies such a no-flux boundary condition. Stationary “shocks” separating multiple targets in unbounded systems provide the same boundary condition. Since the difference between a spiral and a target is not fundamental, the observed spiral breakup must also be due to an *absolute* Eckhaus instability, as described above. This conclusion has important consequences for any quantitative modeling of both the experiments [7] and the simulations [4], and is particularly critical for the computation of the radius of the laminar (i.e., ordered) region of the spiral pattern. Such a computation requires the calculation of the location of the secondary front as a function of the system parameters, as in Fig. 5.

This work was supported in part by the National Science Foundation under Grant No. DMS-9703684. We are grateful to M. Bär and M. Proctor for discussions.

- [1] M.C. Cross and P.C. Hohenberg, *Rev. Mod. Phys.* **65**, 851 (1993).
- [2] P. Couillet, L. Gil, and J. Lega, *Phys. Rev. Lett.* **62**, 1619 (1989).
- [3] L. Kramer, F. Hynne, P. Graae Sorenson, and D. Walgraef, *Chaos* **4**, 443 (1994).
- [4] H. Chaté and P. Manneville, *Physica (Amsterdam)* **224A**, 348 (1996).
- [5] *Chemical Waves and Patterns*, edited by R. Kapral and K. Showalter (Kluwer, Dordrecht, 1995).
- [6] P.S. Hagan, *SIAM J. Appl. Math.* **42**, 762 (1982).
- [7] Q. Ouyang and J.-M. Flesselles, *Nature (London)* **379**, 143 (1996).
- [8] D. Worledge, E. Knobloch, S. Tobias, and M. Proctor, *Proc. R. Soc. London A* **453**, 119 (1997).
- [9] P. Büchel, M. Lücke, D. Roth, and R. Schmitz, *Phys. Rev. E* **53**, 4764 (1996); D. Roth *et al.*, *Physica (Amsterdam)* **97D**, 253 (1996).
- [10] S. Tobias, M.R.E. Proctor, and E. Knobloch, *Physica (Amsterdam)* **113D**, 43 (1998).
- [11] K. Nozaki and N. Bekki, *Phys. Rev. Lett.* **51**, 2171 (1983); A. Weber, L. Kramer, I.S. Aranson, and L. Aranson, *Physica (Amsterdam)* **61D**, 279 (1992).
- [12] P. Couillet, L. Gil, and J. Lega, *Physica (Amsterdam)* **37D**, 91 (1989); H. Sakaguchi, *Prog. Theor. Phys.* **84**, 792 (1990); **85**, 927 (1991).
- [13] I.S. Aranson, L. Aranson, L. Kramer, and A. Weber, *Phys. Rev. A* **46**, R2992 (1992).
- [14] D. Barkley, M. Kness, and L. Tuckerman, *Phys. Rev. A* **42**, 2489 (1990); D. Barkley, *Physica (Amsterdam)* **49D**, 61 (1991). A related model of CO oxidation of Pt(110) also exhibits spiral breakup, see M. Bär and M. Eiswirth, *Phys. Rev. E* **48**, R1635 (1993).